The LINNEAN SOCIETY of London BIOLOGICAL Journal of the Linnean Society

Biological Journal of the Linnean Society, 2014, **113**, 790–804. With 10 figures

A new long-tailed basal bird from the Lower Cretaceous of north-eastern China

ULYSSE LEFÈVRE[1,2]*, DONGYU HU[3,4], FRANÇOIS ESCUILLIÉ[5], GARETH DYKE[6] and PASCAL GODEFROIT[7]

[1]*Department of Geology, University of Liège, allée du 6 Août B18-B20, 4000 Liège, Belgium*
[2]*Department of Paleontology, Royal Belgian Institute of Natural Sciences, rue Vautier 29, 1000 Bruxelles, Belgium*
[3]*Paleontological Institute, Shenyang Normal University, 253 North Huanghe Street, Shenyang 110034, China*
[4]*Key Laboratory of Vegetation Ecology, Ministry of Education, Northeast Normal University, 5268 Renmin Street, Changchun 130024, China*
[5]*Eldonia, 9 avenue des Portes Occitanes, 3800 Gannat, France*
[6]*Ocean and Earth Science, National Oceanography Centre, University of Southampton, Southampton SO14 3ZH, UK*
[7]*Department of Paleontology, Royal Belgian Institute of Natural Sciences, rue Vautier 29, 1000 Bruxelles, Belgium*

Received 18 February 2014; revised 30 April 2014; accepted for publication 30 April 2014; published 17 October 2014

A new basal Avialae, ***Jeholornis curvipes* sp. nov.**, from the Yixian Formation (Lower Cretaceous) of Liaoning Province (north-eastern China) is described. A revision of long-tailed birds from China and a phylogenetic analysis of basal Avialae suggest that Jeholornithiformes were paraphyletic, with *Jixiangornis orientalis* being the sister-taxon of pygostylia. The phylogenetic analysis also recovered that the tail reduction is a unique event in the evolution of birds. *Jeholornis* species were cursorial, nonperching, and seed-eating birds. © 2014 The Linnean Society of London, *Biological Journal of the Linnean Society*, 2014, **113**, 790–804.

ADDITIONAL KEYWORDS: Avialae – Jehol group – *Jeholornis* – Jeholornithiformes – systematic revision.

INTRODUCTION

For more than 150 years, *Archaeopteryx lithographica* remained the only known Mesozoic bird with a long bony tail. Since 1992, however, numerous fairly complete skeletons of long-tailed Mesozoic birds have been discovered, mainly from the Jehol Biota of north-eastern China (Chang *et al*., 2008). Indeed, several clades of basal Avialae are known only from this part of the globe (O'Connor *et al*., 2012).

The first bird specimen from the Jehol biota was described in 1992 as *Sinornis santensis* (Sereno & Rao, 1992). Ten years later, Zhou & Zhang (2002) described *Jeholornis prima*, a basal avialan from the Jiufotang Formation, which is characterized in particular by a long bony tail of 22 caudal vertebrae as in *A. lithographica*. At around the same time, *Shenzhouraptor sinensis* and *Jixiangornis orientalis* were also described: the first from the Jiufotang Formation and the latter from the Yixian Formation. Jeholornithiformes as a group was coined in 2006 (Zhou & Zhang, 2006) to encompass all of the long-tailed birds that are also characterized by a convex rostroventral margin and a concave ventral margin of the dentary (O'Connor *et al*., 2012). This group now includes *J. prima*, *S. sinensis*, *J. orientalis*, *Dalianraptor cuhe*, and *Jeholornis palmapenis* (Zhou & Zhang, 2002; Ji *et al*., 2002a, b; Gao & Liu, 2005; O'Connor *et al*., 2012). Indeed, some studies have suggested that *S. sinensis* and *J. orientalis* might be

*Corresponding author. E-mail: lefevre.u@gmail.com
ZooBank Registration: urn:lsid:zoobank.org:act:882FACA6-CB48-4D5D-ADEE-6E0DAD031101

synonyms of *J. prima* because they are based on juvenile specimens (Zhou & Zhang, 2006; Ji *et al*., 2003; Li *et al*., 2010; Zhou & Wang, 2010).

In the present study, we describe a new specimen of a long-tailed bird from the Yixian Formation placed within Jeholornithiformes. The new specimen provides new information on the anatomy, systematics and phylogeny of this important group of basal birds.

MATERIAL AND METHODS

Geology

The Jehol biota is formed from two formations: the Yixian Formation, dated 124.6 ± 0.3 Mya using U-Pb SHRIMP dating (Yang, Li & Jiang, 2007), and the younger Jiufotang Formation, dated to 120 ± 0.7 Mya using $^{40}Ar/^{39}Ar$ decay (Chang *et al*., 2008). These formations are comprised of lacustrine deposits embedded with volcanic rocks (Jiang *et al*., 2011) and contain the most diversified avifauna known to date closely related to *A. lithographica* (O'Connor *et al*., 2012).

Anatomy

Our use of anatomical nomenclature is applied in accordance with Baumel *et al*. (1993). Although the Latin terminology used by Baumel *et al*. (1993) is retained for muscles, osteological structures are described using the English equivalents of Latin terms (*sensu* Howard, 1929) as is standard in descriptions of non-neornithine fossil birds.

Insitutional abbreviations

IVPP, Institute of Vertebrate Paleontology and Paleoanthropology, Beijing, China; SDM, Shandong Museum, Jinan, China; YFGP, Yizhou Fossil and Geology Park, Yizhou, China.

SYSTEMATIC PALAEONTOLOGY

Dinosauria Owen, 1842

Theropoda Marsh, 1881 *sensu* Gauthier, 1986

Maniraptora Gauthier, 1986

Avialae Gauthier, 1986

Jeholornis Zhou and Zhang, 2002

Type species: Jeholornis prima Zhou and Zhang, 2002

Referred species: Jeholornis palmapenis O'Connor, Sun, Xu, Wang and Zhou, 2012; ***Jeholornis curvipes* sp. nov.**

Revised diagnosis: Pheasant-sized early diverging avialans that share: (i) premaxilla edentulous; (ii) a concave ventral margin and a convex rostro-ventral margin of the dentary; (iii) a straight tibia with a ratio tibia:femur between 1.19 and 1.24; (iv) a nonretroverted caudomedially oriented hallux; (v) a 'J'-shaped first metatarsal; (vi) third metatarsal that is the longest; (vii) penultimate pedal phalanxes not longer than terminal ones; and (viii) each caudal vertebra three or four times as long as wide.

Jeholornis curvipes sp. nov. (Fig. 1)

Holotype: YFGP-yb2, an almost completely articulated skeleton including a partial caudal series (Fig. 1).

Type locality and horizon: Yizhou Fossil and Geology Park, Liaoning Province, (north-eastern China) Dakangpu Member (equivalent to the Dawangzhangzi Beds) of the Yixian Formation, lower Aptian (Lower Cretaceous) (Swisher *et al*., 1999; Yang *et al*., 2007; Chang *et al*., 2009)

Etymology: From the Latin *curvus* (curved) and *pes* (foot), in reference to the lateral deviation of the distal part of the metatarsals in YFGP-yb2.

Diagnosis: This new species of basal bird is characterized by the following features: (i) a dentary without an ossified symphysis; (ii) a strut-like coracoid with a lateral process not detached from the lateral margin; (iii) medial margin of coracoid concave along its entire length; (iv) deltopectoral crest of humerus slightly deflected from the shaft; (v) ratio between metacarpal II and humerus length 0.58 (see Supporting information, Fig. S1); (vi) ratio between metacarpal I and metacarpal II 0.17; (vii) ratio manual phalanx I-1:phalanx II-1 1.29; (viii) the presence of two prominent proximal condyles on the caudal end of the tibia; and (ix) distal half of metatarsals laterally deviated.

Description and comparisons: YFGP-yb2 is an almost complete and articulated skeleton that just lacks the caudal region of the tail (Fig. 1). Also of note, however, is that the rostral part of the skull, the autopodal segment of the right forelimb, and the distal autopodal segment of the right hindlimb were reconstructed during preparation of the specimen. We have confirmed this with X-ray radiographs and so these parts of the skeleton are not described (Fig. 2). X-ray radiography and computed tomography (CT) scans also confirm that YFGP-yb2 is not a chimera in the region of the pelvis as suspected at first examination (see Supporting information, Fig. S2).

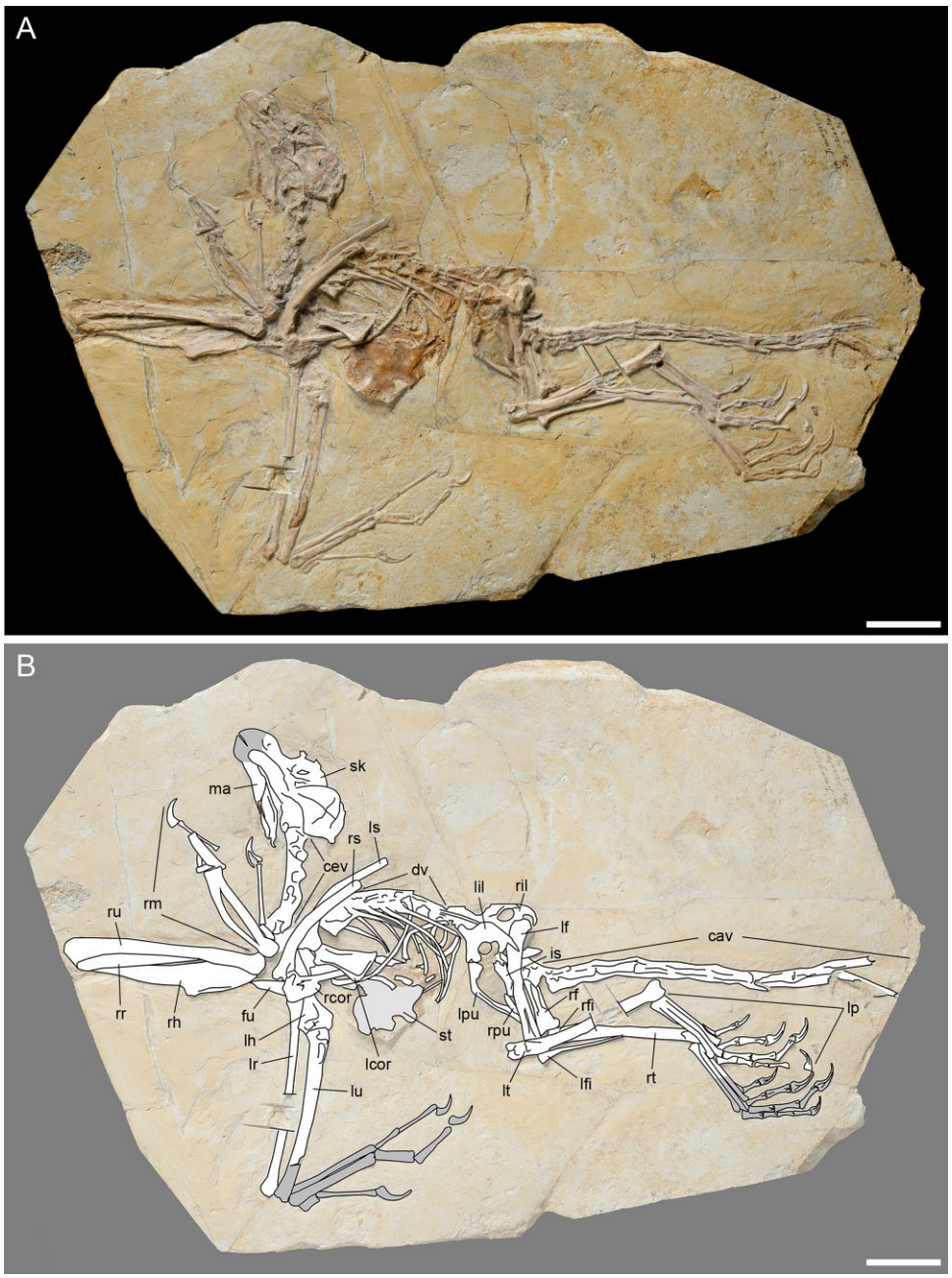

Figure 1. Photograph, drawing and X-ray radiographs of the basal bird ***Jeholornis curvipes*** **sp. nov.**, from the Lower Cretaceous of north-eastern China. A, YFGP-yb2 photograph. B, Line drawing; grey parts represent restored skeletal regions.

Ontogenic stage: The following anatomical features suggest that YFGP-yb2, the holotype of *J. curvipes*, was an adult at death (Forster, 1998; Zhou & Zhang, 2003a; Zhou and Zhang, 2003b; Xu & Norell, 2004; Turner *et al*., 2007; Gao *et al*., 2012; Godefroit *et al*., 2013a): (i) the texture of the bones on the proximal and distal ends of the coracoid, the humerus, the ulna, the pubis, and the femur is regular and continuous; (ii) the frontals are fused together along their sagittal line; (iii) the neural arches of the caudal cervical vertebrae are completely fused to corresponding centra (this suture is not visible in X-rays); (iv) CT scans show that the sacral vertebrae are all fused together; (v) metacarpals II and III are proximally fused; and (v) metatarsals II, III, and IV are proximally fused.

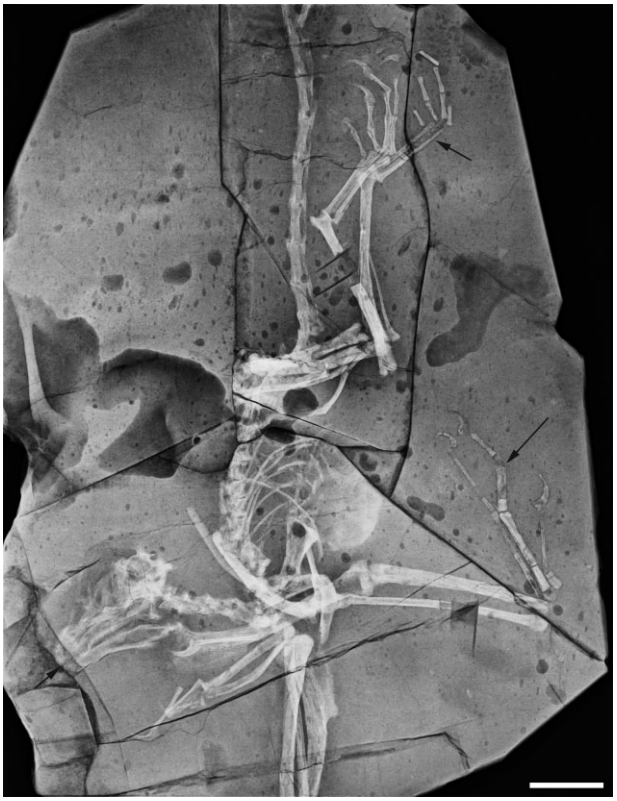

Figure 2. X-ray radiography of YFGP-yb2. Arrows point to reconstructed regions of the specimen (rostral part of the skull, distal part of the left forelimb, and distal part of the right hindlimb). Scale bar = 40 mm.

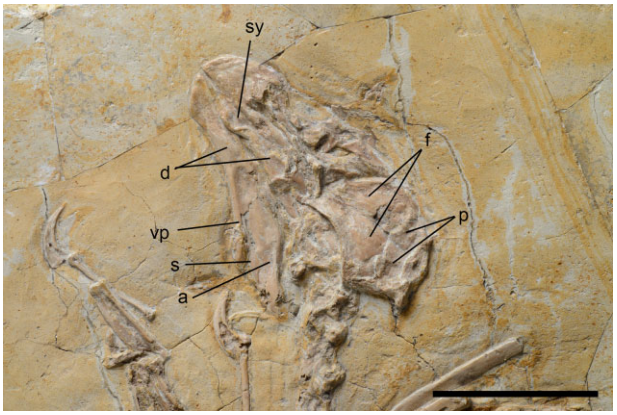

Figure 3. Skull of ***Jeholornis curvipes* sp. nov.**, from the Lower Cretaceous of north-eastern China. a, angular; d, dentaries; f, frontals; p, parietals; s, surangular; sy, symphyseal region; vp, ventral process of the dentary. Scale bar = 40 mm.

Skull: Because the antorbital region is incompletely preserved, it is impossible to check whether this region is rostrocaudally shorter than dorsoventrally high, as in *Xiaotingia zhengi* and other Maniraptora including *A. lithographica* (Xu *et al*., 2011) (Fig. 3). No premaxillary or maxillary fenestrae are preserved as a result of crushing. The frontals are fused together along their whole length and, as in *J. palmapenis* (O'Connor *et al*., 2012), the left frontal is petal-shaped in dorsal view. The frontals are also convex and wider caudally. There is no thickening of the orbital rim, unlike in *Confuciusornis sanctus*, where this thickening is interpreted as the fusion between the palpebral and the frontal (Chiappe *et al*., 1999). The frontals are perpendicularly fused to the parietals, as described for *C. sanctus* (Chiappe *et al*., 1999). Unlike *Mei long*, the interfrontal suture is not separated from the parietals by a triangular notch (Gao *et al*., 2012). The symphysial region of the dentaries is not ossified in contrast to the condition in *J. prima*. The dentaries are robust, as in other members of Jeholornithiformes, with a convex rostroventral margin and a concave ventral margin. The ventral process of the dentary is located under the rostral part of the surangular, whereas the dorsal process is absent. A wide groove extends along the lateral side of the dentary and does not contain any foramina, unlike in Troodontidae and *A. lithographica* (Weishampel, Dodson & Osmólska, 2007; Wellnhofer, 2009). The angular is rostrally thin and becomes wider caudally; the dorsal margin of its rostral end takes part in the ventral edge of the external mandibular fenestra. Dorsal to the angular, there is a wide surangular. The dorsal edge of the surangular is convex and has a groove in its caudal region, which is not prolonged into the rostral region of the same bone. Binocular observations and X-ray radiographs reveal that the jaws are edentulous along their whole preserved length.

Vertebrae: The cervical region of YFGP-yb2 is poorly preserved, making distinction between vertebrae difficult. Although X-ray radiographs allow us to distinguish four unequivocal cervical vertebrae, others are trapped under the scapular region and distinction between the dorsal and the cervical series remains impossible. The most anterior cervical vertebra is 87% craniocaudally shorter than the most caudal cervical vertebrae. The prezygapophyses form a craniomedially oriented articular surface. A cervical rib can be observed in articulation with the second cervical vertebra. This rib is 11.7 mm long, comprising 109% of the length of the corresponding centrum.

X-ray radiographs also reveal eight unequivocal dorsal vertebrae. The anterior part of the dorsal region, however, is crushed under the scapular region and so the most caudal part cannot be distinguished from the sacral region even by X-ray radiographs and CT scans. There is also no size difference between the

eight unequivocal dorsal vertebrae. X-ray radiographs reveal trapezoidal neural spines with dorsal margins that are only slightly shorter than corresponding centra. Neural arches are all completely fused to corresponding centra, which suggests that this specimen is adult (as discussed above).

The sacral region cannot be observed directly because of its poor state of preservation. However, one transverse process that is located caudally to the left femur is as wide as in *J. prima*. This process has a straight lateral margin that forms an angle of less than 45° with the corresponding caudal margin.

Only the first nine caudal vertebrae are preserved. Within this series, proximal centra are 57% shorter than distal ones and the transition point is located after the second caudal vertebrae, as in *J. prima* (Zhou & Zhang, 2002). The neural spines and transverse processes are not visible. Both the proximal and distal articular surfaces of the caudal vertebra are slightly convex. The zygapophyses become longer proximodistally, although their length remains within 30% of the length of the corresponding vertebra. CT scans show that the chevrons of the proximal caudal vertebrae are rectangular and dorsoventrally higher than proximodistally long as in *J. palmapenis*. They become anterocaudally as long as the corresponding centrum in the distal series. As in *A. lithographica*, *Anchiornis huxleyi*, and *Aurornis xui*, a groove extends along the junction between the neural arches and the centrum (Hu *et al*., 2009; Godefroit *et al*., 2013a, 2013b).

Scapular girdle: The scapula is long, thin and ribbon-shaped (Fig. 4). Its distal end is thin and round, as opposed to being sharp as in modern birds (Baumel *et al*., 1993; Chiappe *et al*., 1999; Wellnhofer, 2009). It is ventrally curved and its thickness decreases caudally as in *J. prima* and *S. sinensis* (Ji *et al*., 2002a; Zhou & Zhang, 2002). Its ventral margin is distinctly thicker than its dorsal margin. There is no distal groove near the glenoid fossa at the ventral side of the scapula, as is the case in *X. zhengi* (Xu *et al*., 2011). A prominent acromion process is present on the proximal end of the scapula as in *A. lithographica*, *S. sinensis*, and *Rahonavis ostromi* (Forster, 1998; Wellnhofer, 2009; Ji *et al*., 2003). The glenoid fossa is located caudally to the acromion process and is laterodorsally oriented as in *C. sanctus* (Chiappe *et al*., 1999; Zhou & Zhang, 2003a). The scapula is significantly shorter (66%) than the humerus, as in derived Maniraptora and basal Avialae (Zhang *et al*., 2008) and lies parallel with the dorsal vertebrae as in *A. lithographica* (Wellnhofer, 2009) and *M. long* (Gao *et al*., 2012).

X-ray radiographs reveal a suture between the scapula and the coracoid, indicating that those bones were not completely fused (Fig. 2). The two coracoids contact their respective scapulae at an angle of less than 90°, as in *Zhongjianornis yangi* and *Sapeornis chaoyangensis* (Zhou & Zhang, 2003b; Zhou & Li, 2010). The left coracoid is strut-like as in *J. prima*, *Z. yangi*, and *S. chaoyangensis* (Wellnhofer, 2009) and is approximately half the length of the scapula (Fig. 5). Its sternal margin is sub-horizontal as opposed to being convex as in *J. prima* (Zhou & Zhang, 2002). Its medial margin is clearly concave, whereas it is slightly convex in *J. prima*. The lateral process is not as well developed as in *J. prima*, in which this process is clearly detached from the lateral margin of the coracoid. The procoracoid process is also

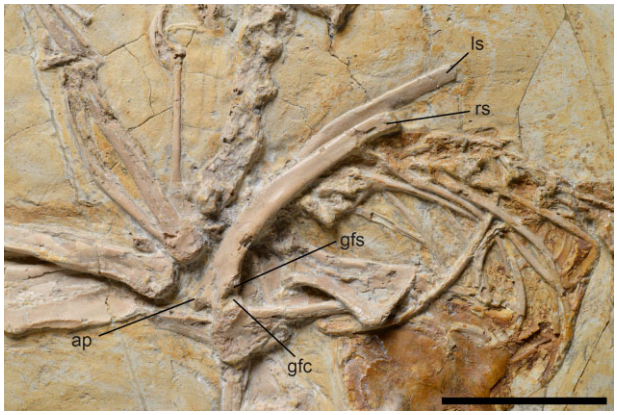

Figure 4. Scapular girdle of ***Jeholornis curvipes* sp. nov.**, from the Lower Cretaceous of north-eastern China. ap, acromial process of scapula; gfc, glenoid fossa of coracoid; gfs, glenoid fossa of scapula; ls, left scapula; rs, right scapula. Scale bar = 40 mm.

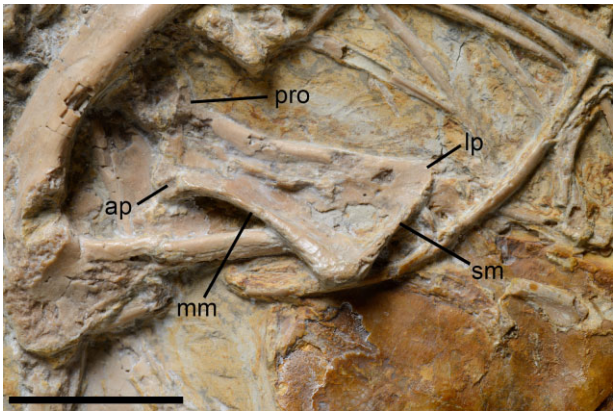

Figure 5. Left coracoid of ***Jeholornis curvipes* sp. nov.**, from the Lower Cretaceous of north-eastern China. ap, acrocoracoid process; lp, lateral process; mm, medial margin; pro, procoracoid process; sm, sternal margin. Scale bar = 40 mm.

poorly developed at the junction between the coracoid and the scapula. A hemispherical acrocoracoid process is prominently developed. There is no subglenoid fossa on the proximal region of the coracoid, unlike the condition in *X. zhengi* and *Eosinopteryx brevipenna* (Godefroit *et al*., 2013b).

The furcula is visible completely on X-ray radiographs. It is robust and boomerang-shaped as in *J. prima*, *A. lithographica*, *C. sanctus*, *X. zhengi*, and Dromaeosauridae (Zhou & Zhang, 2002; Xu *et al*., 2011). The furcula branches are less than one-third of the femur length. There is no hypocleideum at the junction between the two branches, as also seen in *J. prima*, *S. sinensis*, *C. sanctus*, and *A. huxleyi* (Chiappe *et al*., 1999; Norell & Clarke, 2001; Zhou & Zhang, 2002; Ji *et al*., 2003). The intraclavicular angle is 62° and the furcula branches are craniocaudally compressed.

The ribs of YFGP-yb2are long and thin as in many basal birds (e.g. *A. lithographica*, *J. prima*, *S. sinensis*, and *S. chaoyangensis*) and there are no traces of uncinate processes. Elements of gastralia are present near the pelvic region, proximally expanded and tapered distally.

A large brownish element is also present in the sternal region of the skeleton. To determine whether this bone is the remains of the sternum, we performed a scanning electron microscopy (SEM) analysis coupled with energy dispersive spectrometry (EDS). EDS results show that the Ca/P ratio in this region varies between 1.5 and 2 (see Supporting information, Fig. S3), confirming that this element is formed of apatite (Newesely, 1989; Hubert *et al*., 1996). SEM analysis further reveals the presence of concentric lamellar structures, similar to those seen in fresh bones. A Haversian canal and a Volkmann's canal are preserved together with lenticular pores, which lie parallel to the concentric lamellae; these could be the remains of fossilized osteoblasts (Fig. 6A) (Gartner & Hiatt, 2004). Close-up images reveal the presence of mineralized collagen fibres inside a Haversian canal, as also observed in *Iguanodon* bones (Leduc, 2012). It is therefore likely that this brownish element represents the ossified sternum, rarely preserved in basal birds (e.g. *A. lithographica* and *S. chaoyangensis*) (Zhou & Zhang, 2003b). Unfortunately, the poor preservation of this bone prevents further comparisons with other specimens.

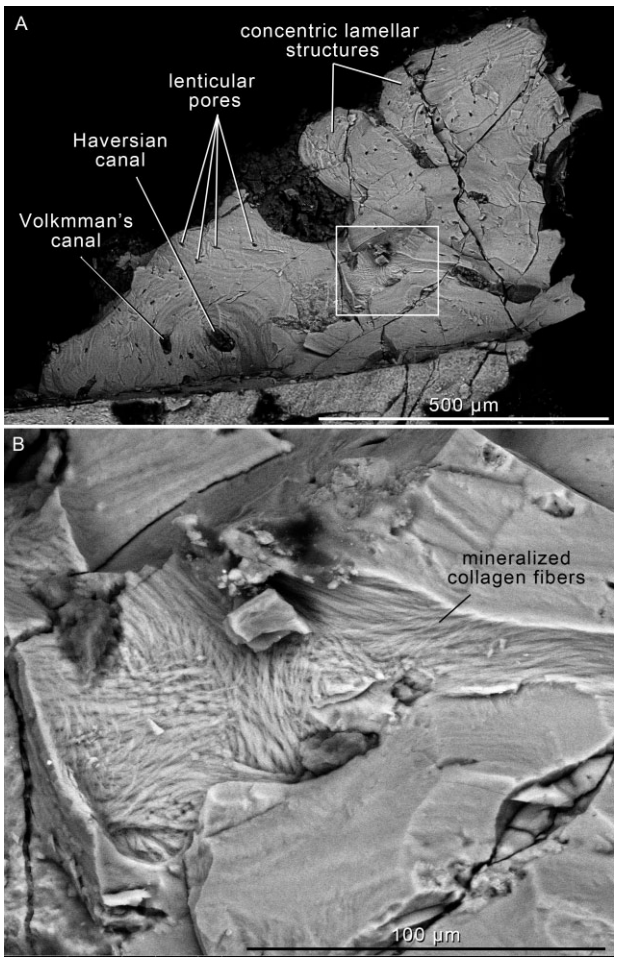

Figure 6. Histological elements from the sternum of ***Jeholornis curvipes* sp. nov.** A, general structure of the bone. B, close-up of mineralized collagen fibres inside a Haversian canal.

Forelimbs: The ratio between forelimb length (humerus + ulna + metacarpal II) and hindlimb length (femur + tibia + metatarsal III) is approximately 1.22, which is similar to the condition observed in *J. prima*.

The humerus is approximately 120% the length of the femur and is more robust. The diaphysis is straight in cranial view (Fig. 7). The deltopectoral crest is wide (117% of the width of the humerus at mid-shaft) and extends along 40% of the humerus length as in *J. prima* and *S. sinensis* (Ji *et al*., 2003). This crest is sub-rectangular as in *J. prima*, *S. sinensis*, and *S. chaoyangensis*. Its dorsal margin is straight as in *S. chaoyangensis*. Its dorsodistal portion does not form an acute angle as in *J. prima*. The humeral head, the bicipital groove, the ventral tubercle, and the pneumotricipital fossa are not visible, even on X-ray radiographs. However, X-ray radiographs clearly reveal the absence of an extended bicipital crest. The distal condyles of the humerus are mainly located on the cranial face of the bone as in *S. chaoyangensis* and advanced birds (Zhou & Zhang, 2003b). The ventral condyle is prominent and ball-shaped, whereas the dorsal condyle is smaller and sub-oval. It is impossible to determine whether these

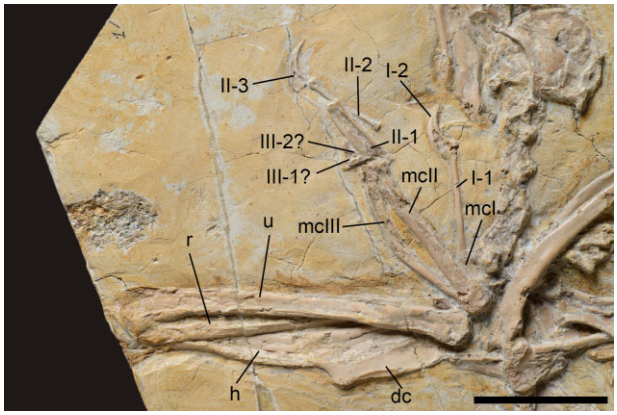

Figure 7. Right forelimb of ***Jeholornis curvipes*** **sp. nov.**, from the Lower Cretaceous of north-eastern China. dc, deltopectoral crest; h, humerus; mc, metacarpal; r, radius; u, ulna. Scale bar = 40 mm.

two condyles are caudally separated by the olecranon as in *M. long* (Gao *et al*., 2012). Proximally to these two condyles lies a slight depression, which can be interpreted as the coronoid fossa for insertion of the brachialis muscle. The entepicondyle and ectepicondyle are incompletely preserved. Unlike *C. sanctus*, the proximal part of the humerus is not fenestrated (Chiappe *et al*., 1999; Zhou & Zhang, 2003a).

The ulna is slightly longer than the humerus (106% of the humeral length) as in *S. sinensis* and *S. chaoyangensis*, whereas it is exactly the same length in *J. prima* (Zhou & Zhang, 2002; Ji *et al*., 2002a; Pu *et al*., 2013). The diaphysis is slightly curved dorsally as in *J. prima*, *S. sinensis*, *Yandangornis longicaudus*, *M. long*, *Zhongjianornis elegans*, *R. ostromi*, and *Epidexypteryx hui* (Forster, 1998; Cai & Zhao, 1999; Zhou & Zhang, 2002; Ji *et al*., 2002a; Zhang *et al*., 2008; Zhou & Li, 2010; Gao *et al*., 2012). The proximal portion of the right ulna bears a flat and oval surface probably for the insertion of the brachialis muscle.

The radius is slightly shorter (97%) than the humerus. The diaphysis of the left radius is expanded as in *C. sanctus*, although it is impossible to know if this expansion forms a rectangular transverse surface for articulation with the radial. Although a groove extends along the total length of the radius, this is interpreted as the result of crushing and so cannot be compared with the similar and characteristic groove present in enanthiornithines (Chiappe *et al*., 1999).

The manus (here, the combined length of metacarpal II + phalanx II-1 + phalanx II-2 + ungual II) is longer than the humerus (123%). Metacarpal I is rectangular and is not fused to metacarpal II as in *C. sanctus* (Chiappe *et al*., 1999), whereas metacarpal I is extremely short (1/16 of the metacarpal II length) as in *J. prima*. Metacarpal II is straight and as wide as metacarpal III, whereas the proximal end of metacarpal II terminates at the same level as metacarpal III, unlike in *C. sanctus* and *S. chaoyangensis* (Chiappe *et al*., 1999; Pu *et al*., 2013). Metacarpals II and III are fused proximally and form a prominent carpal trochlea as in *J. prima*, *C. sanctus*, *S. chaoyangensis*, and *Z. elegans* (Cai & Zhao, 1999; Chiappe *et al*., 1999; Zhou & Zhang, 2003b; Zhou & Li, 2010). Metacarpals II and III are also fused distally and form a ginglymoid articular surface as in *J. prima* and *M. long* (Zhou & Zhang, 2002; Gao *et al*., 2012). X-ray radiographs confirm the total fusion of both the proximal and distal ends of metacarpals II and III, with a complete absence of a suture line between these bones. Metacarpal III is bowed as in *J. prima* and *S. sinensis* (Zhou & Zhang, 2002; Ji *et al*., 2002a) and the interosseous space is as wide as the ulna at midshaft.

The phalangeal formula of YFGP-yb2 is 2-3-3/4-X-X. The penultimate phalanx and the ungual of digit III are only discernable on X-ray radiographs. Thus, it is impossible to determine the exact number of phalanxes for this finger. Phalanx I-1 does not reach the distal end of metacarpal II as in *S. sinensis*, *J. prima*, *S. chaoyangensis*, *C. sanctus*, enantiornithines, and ornithurines (Zhou & Zhang, 2003a, b; Ji *et al*., 2003). This phalanx is straight and thin (one-third of the width of phalanx II-1). Ungual I is slightly shorter than ungual II, unlike in *S. sinensis*. Phalanx II-1 is the most robust phalanx of the manus as in *J. prima*, *S. sinensis*, and *S. chaoyangensis* (Zhou & Zhang, 2002; Ji *et al*., 2002a; Pu *et al*., 2013). The length of phalanx II-1 is approximately half the length of phalanx II-2, unlike in *S. sinensis* where phalanx II-1 is approximately the same length as the phalanx II-2 (Ji *et al*., 2002a). Phalanx II-2 is as long as phalanx II-1 but three times thinner than the latter, whereas the width of phalanx II-2 is constant along its length. Ungual II is the largest in the manus. It is not more curved than unguals I and III. It is impossible to determine whether phalanges III-1 and III-2 formed an angle as in *S. sinensis* (Ji *et al*., 2003). Ungual III is the smallest and is only visible under X-ray. No flexor tubercle can be seen and a deep pit for the insertion of the collateral ligament is present at the level of the distal end of phalanx II-2.

Pelvic girdle: This region has been highly crushed during fossilization (Fig. 8). The right ilium is 44% the length of the femur and its dorsal margin is broken off. CT scans show that the dorsal margin of the left ilium was reconstructed during fossil preparation: slices clearly show that compact bone surrounding the

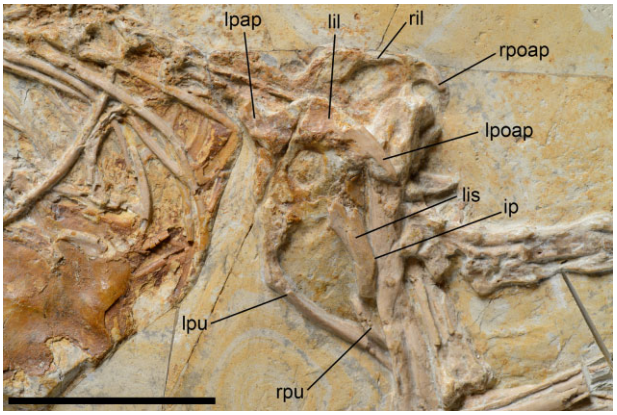

Figure 8. Pelvic girdle of ***Jeholornis curvipes*** **sp. nov.**, from the Lower Cretaceous of north-eastern China. ip, intermediate process of ischium; lil, left ilium; lis, left ischium; lpu, left pubis; lpap, left preacetabular process of ilium; lpoap, left postacetabular process of ilium; ril, right ilium; rpoap, right postacetabular process of the ilium; rpu, right pubis. Scale bar = 40 mm.

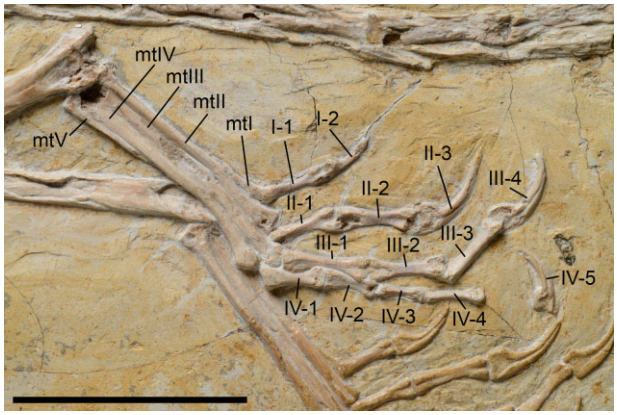

Figure 9. Hindlimb of ***Jeholornis curvipes*** **sp. nov.**, from the Lower Cretaceous of north-eastern China. mt, metatarsal. Scale bar = 40 mm.

spongy bone is missing (see Supporting information, Fig. S4). 3D reconstruction of the pelvic girdle of YFGP-yb2 shows that the distal part of the dorsal margin is regularly convex. CT scans also show that the preacetabular process is partly reconstructed. There is no trace of a brevis fossa as seen in *C. sanctus*. The left pubis is twisted and broken off. CT scans show that the right pubis is slightly sigmoidal and terminates into a spoon-shaped pubic foot with a posterior process as long as the distal width of the femur. The anterior process of the pubic foot is absent. The 3D reconstruction also shows that the pubic symphysis was not ossified. It is impossible to determine how far the pubic symphysis extended as a result of displacement of the two bones. Only the left ischium is preserved. Its distal proximal part is badly defined, making the measurement of the total length impossible. Its distal part has no ventrodistal and dorsodistal processes. Only the intermediate process is located at mid-shaft and does not project as far caudally as in *A. lithographica* (Wellnhofer, 2009).

Hindlimbs: The left hindlimb is well-preserved and covers the right one (Fig. 9). The femur is 20% shorter than the tibia and its proximal half is slightly bowed laterally as in *S. chaoyangensis*, *C. sanctus*, *A. xui*, and *S. sinensis* (Chiappe *et al*., 1999; Ji *et al*., 2002a; Pu *et al*., 2013; Godefroit *et al*., 2013a). The proximal half of the femur is narrower than its distal half, as in *S. chaoyangensis*, *Buitreraptor gonzalezorum* (Makovicky, Apesteguía & Agnolín, 2005), *R. ostromi*, and *A. huxleyi*. The femoral head is sub-oval and is not separated from the trochanteric region by a distinct neck, contrary to what can be seen in *C. sanctus*. CT scans reveal that the fossa for the capital ligament is absent at the top of both femoral heads, resembling the condition in *R. ostromi*, *Z. elegans*, and *A. lithographica* (Forster, 1998; Wellnhofer, 2009; Zhou & Li, 2010). The greater trochanter is not prominent and is hardly discernible from the femoral shaft. An oval area, the position of which corresponds to that of fourth trochanter, is present along the caudal side of the femur (Weishampel *et al*., 2007; Lu *et al*., 2009). Distally, the medial and the lateral condyles are caudally developed and, unlike in *Y. longicaudus*, the medial condyle is wider than the lateral one. The fibular trochlea is well developed on the lateral condyle, whereas the tibiofibular crest is poorly preserved. The intercondylar sulcus is narrower than the lateral condyle. The popliteal fossa is not as deep as in *A. lithographica*, *R. ostromis*, and *J. prima* (Forster, 1998; Zhou & Zhang, 2002; Wellnhofer, 2009). The tibia is straight as in *S. sinensis*, *C. sanctus*, *R. ostromi*, and *M. long* (Forster, 1998; Chiappe *et al*., 1999; Ji *et al*., 2002a; Gao *et al*., 2012). This bone is as wide as the femur as in *J. prima*, *J. palmapenis*, and *S. sinensis* (Zhou & Zhang, 2002; Ji *et al*., 2002a; O'Connor *et al*., 2012). There is no trace of a cnemial crest at the proximal part of the bone as in many basal birds. The caudal side of the tibia shows two prominent condyles surroundering a deep fossa for insertion of the flexor muscle. The fibular crest is laterally located and extends over one-ninth of the length of the tibia. Distally, the medial condyle is as wide as the lateral condyle, as in *S. chaoyangensis*, whereas, in non-avian theropods, the medial condyle is wider than the lateral one (Chiappe *et al*., 1999).

The left fibula lies on its medial face and is identical to that of *Jeholornis* specimens in having a wide

proximal part that rapidly tapers distally. This bone is half the length of the tibia and shows a proximocranial process that projects anteriorly.

The left pes lies on its dorsal side. There are five metatarsals as in *A. lithographica*, *C. sanctus*, *S. chaoyangensis*, *J. prima*, *J. palmapenis*, and *S. sinensis* (Chiappe *et al*., 1999; Zhou & Zhang, 2002; Ji *et al*., 2002a; Wellnhofer, 2009; O'Connor *et al*., 2012; Pu *et al*., 2013). Metatarsal V is reduced to less than one-third the length of metatarsal IV. The proximal part of the five metatarsals is straight, whereas the distal part is bent laterally. This configuration of the metatarsals is not artefactual because X-ray radiographs do not show any fracture or counterfeits. The metatarsals are fused proximally, together with the distal tarsals. They are not fused distally and there are no vascular foramina in this area, unlike in *C. sanctus* and *S. choayangensis*, and modern birds (Baumel *et al*., 1993; Chiappe *et al*., 1999; Zhou & Zhang, 2003b).

Metatarsal I is 'J'-shaped in ventral view with a sharp proximal end and a wider distal end as in *X. zhengi*, *C. sanctus*, and *Z. elegans* (Chiappe *et al*., 1999; Zhou & Li, 2010; Xu *et al*., 2011). Its distal trochlea does not align distally with the distal trochlea of the other metatarsals. It lays in the same direction as metatarsals II–IV, suggesting that metatarsal I dorsolaterally articulated with metatarsal II as in *S. sinensis*, *J. palmapenis*, *C. sanctus*, *A. huxleyi*, *E. brevipenna*, *A. lithographica*, and *A. xui* (Chiappe *et al*., 1999; Ji *et al*., 2002a; Hu *et al*., 2009; Wellnhofer, 2009; O'Connor *et al*., 2012; Godefroit *et al*., 2013a, 2013b) Metatarsal III is the largest and reaches half the length of the tibia. Its proximal part is not pinched as in the arctometatarsalian condition. Metatarsals II and III terminate in a ginglymoid articulation, whereas the metatarsal IV terminates, as in *C. sanctus*, with a rounded, laterally-compressed condyle.

The phalangeal formula is 2-3-4-5-0(X). Digit I is short and does not reach the proximal end of the distal trochlea of phalanx II-2. Phalanx II-2 is longer than phalanx II-1, as in *Microraptor gui* and all the basal avialans (Zhou & Zhang, 2002). Unlike Dromaeosauridae and Troodontidae, phalanx II-2 is not reduced in length and does not show a prominent proximoventral heel (Xu *et al*., 2011). In all the digits, the penultimate phalanx is longer than the others. The flexor tubercles are not well developed, as in *J. prima* (Zhou & Zhang, 2003a). The width of digits II and III is constant, whereas the width of digit IV decreases proximodistally. The unguals are broad and curved; the ungual of digit II is slightly longer than that of digit III. The ungual groove is centered on the lateral side of each unguals. The proximoventral heel of each ungual is more developed than the proximodorsal one.

Body mass estimation: Graphic double integration (Seebacher, 2001) cannot be applied for estimating the body mass of *J. curvipes* because of mediolateral crushing of the fossil. A more empirical method, based on the work of Christiansen & Farina (2004), is used in the present study. This method gives a body mass of 0.59 kg, which is consistent with the body mass estimate of *J. prima* (see Supporting information, Fig. S5).

DISCUSSION

Comparisons with other Jeholornithiformes

YFGP-yb2 shares with all species referred to Jeholornithiformes the presence of a robust dentary with a convex rostroventral margin and a concave ventral margin. However, this character cannot be regarded as diagnostic for the group because it is also present in *S. chaoyangensis*, Oviraptorosauria, and Therizinosauroidea (Zhou & Zhang, 2002; O'Connor *et al*., 2012).

Dalianraptor cuhe is not considered for comparisons because it requires further preparation to clarify its anatomy and systematic position (O'Connor *et al*., 2012).

Shenzhouraptor sinensis and *J. prima* share the following characters (Table 1) (Ji *et al*., 2003): (i) robust mandibles with ossified symphyses; (ii) typical U-shaped furculae; (iii) a lachrymal with two vertical and elongated pneumatic fossa; (iv) a ratio of forelimb to hindlimb length of approximately 1.2–1.27; (v) the deltopectoral crest extends along 41% of the humeral length; (vi) the phalanx II-1 is very wide; (vii) the phalanx III-1 is twice as long as the phalanx III-2; (viii) the flight feathers are distinctly longer than the total length of both ulna and manus; (ix) a long tailed composed of 23 or more caudal vertebrae; and (x) the length of each vertebra is three to four times its width. However, the number of caudal vertebrae is at first sight different in both taxa: 23–25 in *Shenzhouraptor*, 27 in *J. prima* IVPP 13274, and 24 in *J. prima* IVPP V13353 (Ji *et al*., 2003; Zhou & Zhang, 2003a; Zhou and Zhang, 2002). However, this difference cannot be regarded as diagnostic because considerable intraspecific variation in the number of caudal vertebrae is reported in *A. lithographica* and *S. chaoyangensis*, although the number of cervical vertebrae and dorsal vertebrae is relatively constant (Berger, 1956; Webster & Goff, 1977; Zhou & Zhang, 2003b; Mayr *et al*., 2007; Pu *et al*., 2013). The absence of teeth in *S. sinensis* cannot be considered as a character that differs from *J. prima* because the skull and mandibles are poorly preserved (Ji *et al*., 2003). We therefore regard *S. sinensis* as a synonym of *J. prima sensu* Ji *et al*. (2003), Zhou & Zhang (2006), Li *et al*. (2010) and Zhou & Wang (2010).

Table 1. Character comparisons within Jeholornithiformes

Character	*Shenzhouraptor sinensis*	*Jeholornis prima*	*Jeholornis palmapenis*	*Jeholornis curvipes*	*Jixiangornis orientalis*
Robust mandibles with ossified symphysis	?	Yes	Yes	Yes	Yes
Typical U-shaped furcula	Yes	Yes	?	No	?
Lachrymal with two elongated pneumatic fossa	Yes	Yes	?	Yes	Yes
Ratio of forelimb to hindlimb length	1.2–1.27	1.2	?	1.23	1.35
The deltopectoral crest extends along of the humeral length	41%	41%	?	40%	38%
The phalanx II-1 is very wide	Yes	Yes	?	Yes	Yes
The phalanx III-1 twice as long as the phalanx III-2	Yes	Yes	?	?	?
The flight feathers disctinctly longer than the total length of both ulna and manus	Yes	?	?	?	?
The length of each caudal vertebra is three to four times its width	Yes	Yes	Yes	Yes	Yes
A toothed maxillary	No	No	Yes	No	No
Thoracic vertebra laterally excavated proximally by two fenestra that converge centrally and forming a single lateral opening in the caudalmost thoracics	No	?	Yes	?	?
The dorsal margin of ilium strongly convex	No	No	Yes	No	No
Post-acetabular wing of the ilium strongly concave ventrally	No	No	Yes	No	?
Ischium curved dorsally	No	No	Yes	?	No
The presence of a large one-piece sternum with a faint keel	No	No	Yes	?	Yes
Metatarsals	5	5	5	5	4
Strut-like coracoid with a lateral process not detached from the lateral margin	No	No	?	Yes	No
Medial margin of coracoid concave along its entire length	?	No	?	Yes	No
Sternal margin of the coracoid sub-horizontal	?	No	?	Yes	No
Deltopectoral crest less deflected from the shaft of the humerus	No	No	?	Yes	No
Ratio metacarpal II to humerus length	0.46	0.43	?	0.58	0.40
Ratio metacarpal I to metacarpal II length	?	0.28	?	0.17	0.25
Ratio manual phalanx I-1 to phalanx II-1 length	?	1.12	?	1.29	1.23
Presence of two prominent condyles at the caudal side of the tibia projecting far posteriorly	No	No	No	Yes	No
Distal half of metatarsals with a lateral deviation	No	No	No	Yes	No

Many characters considered diagnostic to *S. sinensis* are also found in *J. curvipes* (Table 1) but many others characters also distinguish *J. curvipes* from *S. sinensis* (see *J. curvipes* diagnosis, above). Comparing *J. palmapenis* and *S. sinensis* is more difficult because *J. palmapenis* does not preserve its scapular girdle and its forelimbs.

Jeholornis palmapenis is well characterized by the following autapomorphies that are not found in *J. prima*, *J. curvipes*, and *J. orientalis*. This taxon is therefore regarded as a valid species rather than a synonym of *J. prima* (Table 1): (i) a toothed maxillary; (ii) thoracic vertebra laterally excavated proximally by two fenestra that converge centrally and forming a single lateral opening in the caudalmost thoracics; (iii) dorsal margin of ilium strongly convex; (iv) post-acetabular wing of the ilium strongly concave ventrally; and (v) ischium curved dorsally (O'Connor *et al*., 2012).

Jixiangornis orientalis also has characters that are unique among Jeholornithiformes, including: (i) the presence of a large single-element sternum with a faint keel; (ii) ratio of forelimb to hindlimb length of 1.31, and (iii) a deltopectoral crest that extends less than 40% of the humeral length. The presence of four metatarsals in *J. orientalis* is an other character that can be used to distinguish it from *J. prima*, *J. palmapenis*, and *J. curvipes*.

Several characters also clearly differentiate *J. curvipes* from the other members of Jeholornithiformes (Table 1): (i) dentary without ossified symphysis contrary to what is seen in *J. prima* and *S. sinensis* (in *J. palmapenis*, the dentaries appear to be unfused rostrally, as in *J. curvipes*, although the region is very poorly preserved; O'connor *et al*., 2012); (ii) strut-like coracoid with a lateral process not detached from the lateral margin, contrary to *J. prima*; (iii) medial margin of coracoid concave along its entire length (this is straight to slightly convex in *J. prima* and *J. orientalis*); (iv) sternal margin of the coracoid sub-horizontal and not convex as in *J. prima* and *J. orientalis*; (v) deltopectoral crest less deflected from the shaft of the humerus than in *J. prima*, *S. sinensis*, and *J. orientalis*; (vi) ratio between metacarpal II to humerus length of 0.58, greater than *J. prima*, *S. sinensis*, and *J. orientalis* (0.43, 0.46, and 0.40, respectively); (vii) ratio metacarpal I to metacarpal II length 0.17, smaller than *J. prima* and *J. orientalis* (0.28 and 0.25, respectively); (viii) ratio manual phalanx I-1 to phalanx II-1 length of 1.29, slightly greater than *J. orientalis* (1.12) but closer to *J. prima* (1.23); (ix) the presence of two prominent proximal condyles on the caudal side of the tibia that project further posteriorly than in the other species, and (x) distal half of metatarsals with a lateral deviation unique within Jeholornithiformes. These ten characters distinguish *J. curvipes* from all previously described specimens.

Phylogenetic analysis

A phylogenetic analysis was conducted to assess the relationships of *J. curvipes* within Avialae. Although several phylogenies of Avialae have been proposed (Xu & Norell, 2004; Xu & Zhang, 2005; Hu *et al*., 2009; Xu *et al*., 2009; Xu *et al*., 2011; Lee & Worthy, 2012), our analysis is based on the data matrix published by Godefroit *et al*. (2013a). The *Shenzhouraptor* operational taxonomic unit (OTU) was removed from the original matrix because it included all species referred to the genus *Jeholornis*, and three new OTUs were included, *J. prima*, *J. palmapenis*, and *J. curvipes*. Our new matrix now includes 103 OTUs for 991 informative characters. The results of our phylogenetic analysis are presented in Figure 10, with focus on Avialae. The character distribution for the three new taxa added to the original matrix is presented in the Supporting information (Fig. S6).

Nine hundred and ninety-one characters were equally weighted and analyzed with TNT, version 1.1 (Goloboff, Farris & Nixon, 2008). A heuristic search of 1000 replicates using random addition sequences, followed by branch swapping by tree-bisection–reconnection (holding ten trees per replicate) was conducted. The trees were subsequently analyzed using WINCLADA, version 1.00.08 (Nixon, 2002). Bremer support was assessed by computing decay indices with TNT, version 1.1.

The maximum parsimony analysis resulted in a single tree of 4570 steps. The consistency index is 0.26 and the retention index is 0.54. The consensus tree together with its description is presented in the Supporting information (Fig. S7). Species referred to Jeholornithiformes occupy a position within Avialae confirming their status as basal birds. *Jeholornis prima*, *J. palmapenis*, and *J. curvipes* form a clade supported by nine homoplasious synapomorphies: (i) the dorsoventral process of the dentary is ventrally bowed (character 1359 [1]); (ii) the anteroposterior length of the pre-acetabular process is less than the anteroposterior length of the post-acetabular process (character 398 [0]); (iii) the length of the pre-acetabular process does not reach 6/5th of its proximal dorsoventral height (character 803 [0]); (iv) the proximodistal length of the post-acetabular process comprises between 2/5th and all of the space between the pre-acetabular and post-acetabular embayement of the bone (character 1055 [1]); (v) the distal end of the ischial peduncle in lateral view is a broad and flat articular surface (character 628 [1]); (vi) the ratio of the dorsoventral depth to the basal anteroposterior

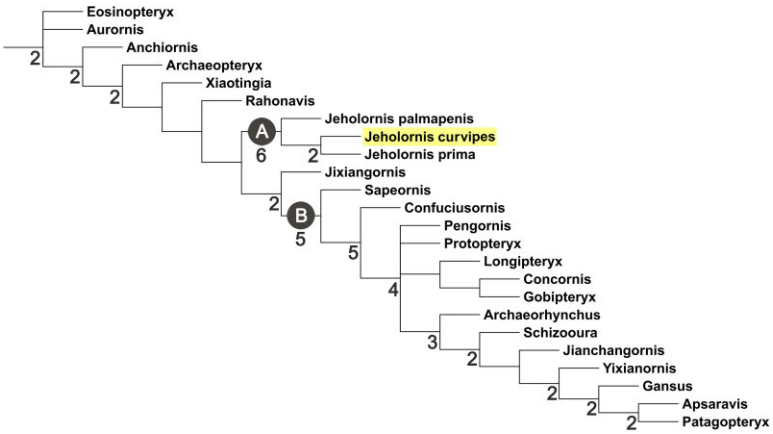

Figure 10. Strict consensus tree resulting from our phylogenetic analysis (length = 4570, consistency index = 0.26, retention index = 0.54). Only clade Avialae is presented (for the complete consensus tree, see the Supporting information, Fig. S7). A, Jeholornithiformes. B, pygostylia. Bremer support values superior to 1 are indicated next to the internodes.

length of the pubic peduncle comprises between 1 and 1/2th (character 1143 [1]); (vii) the tibiofibular crest at the distal end of the femur is sharply demarcated from the fibular condyle by a sulcus or a concavity (character 735 [1]); (viii) the distal half of the femur is as thick as its proximal half (character 1093 [0]), and (ix) the distal extensor pits of the pedal phalanges are deep with defined margins (character 1450 [1]). These nine homoplasious synapomorphies can be used to redefine the genus *Jeholornis*. The *J. prima* + *J. curvipes* clade is supported by three homoplasious synapomorphies, namely: (i) the anterior surface of the cervical and anterior dorsal vertebrae centra is moderately convex (character 194 [1]); (ii) the shape of chevrons for the middle caudal vertebrae represents a hyperelongated processes, longer than two times adjacent centra (character 355 [4]), and (iii) the posteroventral surface of the dentary for the symphysis is present and prominent (character 1240 [1]).

In our phylogeny, *J. orientalis* is the sister-taxon to the pygostylian lineage, as already recovered by Turner, Makovicky & Norell (2012). The two lineages share these synapomorphies: (i) the anteroposterior diameter of the external mandibular fenestra is subequal or longer than one-quarter of the length of the mandible (character 171 [1]); (ii) seven sacral vertebrae have their transverse processes in articulation with the medial wall of the iliac blades (character 343 [5]); (iii) the proximodistal length of the tibia comprises between 1 and 6/5 (character 460 [1]); (iv) metatarsals are proximally fused together (character 476 [1]); (v) the distalmost extent of the laterodistal end of the tibia is distally placed to the distal extent of the mediodistal end (character 561 [1]); (vi) the sternal plates are ossified (character 1037 [1]), and (vii) the presence of a hypocleidum at the junction of the branches of the furcula (character 1385 [1]). As previously discussed, Jeholornithiformes (*J. prima*, *J. palmapenis*, *S. sinensis*, and *J. orientalis*) is paraphyletic. *Jixiangornis orientalis* should no longer be considered as a member of Jeholornithiformes because its phylogenetic position is closer to the pygostylians than to *J. prima*. By contrast to the study of Zhou & Li (2010) and Turner *et al*. (2012), *S. chaoyangensis* is recovered here as the most basal pygostylian. The position of this taxon suggests that the reduction of the tail into a pygostyle was a unique event in the evolution of birds as has been suggested by previous studies (Chiappe & Witmer, 2002; Zhou & Zhang, 2002; Gao *et al*., 2008; Godefroit *et al*., 2013a).

Paleoecology

All of the species referred to *Jeholornis* are characterized by a robust triangular dentary, likely related to their granivorous diet (Zhou & Zhang, 2002). *Jeholornis curvipes* has shorter penultimate pedal phalanges, as has *J. prima*, *J. palmapenis*, and nonperching birds (Zhang *et al*., 2002); species referred to the genus *Jeholornis* therefore probably had terrestrial habits (Zhang *et al*., 2002). The absence of a reversed hallux in *Jeholornis* supports this hypothesis (O'Connor, Chiappe & Bell, 2011). In *J. prima* and *J. palmapenis*, the rectrices taper distally and do not overlap significantly proximally and distally so no airfoil is formed. Such plumage, which resembles the configuration in *Caudipteryx zoui* (Dyke & Norell, 2005), is possibly related to a visual display function (Zhou & Zhang, 2003b; O'Connor *et al*., 2012). Recent accurate observations of *J. prima*

and *J. palmapenis* have highlighted a fan-shaped tract of feathers above the proximal caudal vertebrae. This tract appears to be more implicated in ornamentation than in flight (O'Connor *et al*., 2013).

In view of our results, it is likely that the genus *Jeholornis* only includes terrestrial and seed-eating birds, although quantitative analyses are necessary to understand the aerodynamic capacity of these basal birds.

CONCLUSIONS

The genus *Jeholornis* encompasses three species: *J. prima* (Zhou & Zhang, 2002), *J. palmapenis* (O'Connor *et al*., 2012), and ***J. curvipes* sp. nov.** *Shenzhouraptor sinensis* is here considered as a junior synonym of *J. prima*. Our phylogenetic analysis shows that *J. orientalis* is not a member of the Jeholornithiformes but the sister-taxon to the pygostylians. This position is supported by seven homoplasious synapomorphies, although further investigation of the specimen will be required to fully determine its phylogenetic position. Our phylogenetic analysis also corroborates the suggestion that the reduction of the tail into a pygostyle was a unique event in the evolution of birds. The presence of a nonreversed caudomedially positioned hallux and a unique caudal plumage combined with a phalangeal proportion that are not characteristic for perching birds indicate that the *Jeholornis* species were most likely terrestrial, seed-eating birds.

ACKNOWLEDGEMENTS

We thank A. Cau for discussions and information about the phylogenetic matrix and C. Moors who helped to define the species name. We thank T. Hubin for photographs. We also thank M. Mortimer and X. Wang for their help with earlier iterations of this manuscript and three anonymous reviewers for their helpful comments.

REFERENCES

Baumel JJ, King AS, Breazile JE, Evans HE, Vanden Berge JC. 1993. *Handbook of avian anatomy: nomina anatomica avium*, 2nd edn. Cambridge, MA: The Nuttall Ornithological Club.

Berger A. 1956. Anatomical variation and avian anatomy. *Condor* **58:** 433–441.

Cai Z, Zhao L. 1999. A long tailed bird from the Late Cretaceous of Zhejiang. *Science in China* **42:** 434–441.

Chang MM, Chen PJ, Wang YQ, Wang Y, Miao D. 2008. *The Jehol fossils: the emergence of feathered dinosaurs, beaked birds and flowering plants*. Amsterdam: Academic Press.

Chang S, Zhang H, Renne PR, Fang Y. 2009. High-precision 40Ar/39Ar age for the Jehol biota. *Palaeogeography, Palaeoclimatology, Palaeoecology* **280:** 94–104.

Chiappe LM, Norell MA, Ji Q, Ji S. 1999. Anatomy and systematics of the confuciusornithidae (Theropod: Aves) from the late Mesozoic of northeastern China. *American Museum of Natural History* **242:** 1–89.

Chiappe LM, Witmer LM. 2002. *Mesozoic birds: above the heads of dinosaurs*. London: University of California Press.

Christiansen P, Farina RA. 2004. Mass prediction in theropod dinosaurs. *Historical biology* **16:** 85–92.

Dyke GJ, Norell MA. 2005. *Caudipteryx* as a non-avialan theropod rather than a flightless bird. *Acta Palaeontologica Polonica* **50:** 101–116.

Forster CA. 1998. The theropod ancestry of birds: new evidence from the Late Cretaceous of Madagascar. *Science* **279:** 1915–1919.

Gao CL, Chiappe LM, Meng QJ, O'Connor JK, Wang XR, Cheng XD, Liu JY. 2008. A new basal lineage of Early Cretaceous birds from China and its implications on the evolution of the avian tail. *Palaeontology* **51:** 775–791.

Gao CL, Liu JY. 2005. A new avian taxon from Lower Cretaceous Jiufotang Formation of western Liaoning. *Global Geology* **24:** 313–316.

Gao CL, Morschhauser EM, Varrichio DJ, Liu J, Zhao B. 2012. A second soundly sleeping dragon: new anatomical details of the Chinese troodontid *Mei long* with implications for phylogeny and taphonomy. *PloS ONE* **7:** e45203.

Gartner PL, Hiatt JL. 2004. *Atlas en couleur d'histologie*, 2nd edn. Paris: Edition Pradel.

Gauthier J. 1986. Saurischian monophyly and the origin of birds. *Memoirs of the California Academy of Sciences* **8:** 1–55.

Godefroit P, Cau A, Hu DY, Escuillié F, Wu W, Dyke G. 2013a. A Jurassic avialan dinosaur from China resolves the early phylogenetic history of birds. *Nature* **498:** 359–362.

Godefroit P, Demuynck H, Dyke G, Hu D, Escuillié F, Claeys P. 2013b. Reduced plumage and flight ability of a new Jurassic paravian theropod from China. *Nature Communications* **4:** 1394.

Goloboff P, Farris J, Nixon K. 2008. TNT, a free program for phylogenetic analysis. *Cladistics* **24:** 774–786.

Howard H. 1929. The avifauna of Emeryville Shellmound. *University of California Publications in Zoology* **32:** 301–394.

Hu D, Hou L, Zhang L, Xu X. 2009. A pre-*Archaeopteryx* troodontid theropod from China with long feathers on the metatarsus. *Nature* **461:** 640–643.

Hubert JF, Panish PT, Chure DJ, Prostak KS. 1996. Chemistry, microstructure, petrology and diagenetic model of Jurassic dinosaur bones, Dinosaur National Monument, Utah. *Journal of Sedimentary Research* **66:** 531–547.

Ji Q, Ji S, You H, Zhang J, Yuan C, Ji X, Li J, Li Y, By T, Downs W. 2002a. Discovery of an Avialae bird from China, *Shenzhouraptor sinensis*. *Geological Bulletin of China* **21:** 363–369.

Ji Q, Ji S, You H, Zhang J, Zhang H, Zhang N, Yuan C, Ji X. 2003. An early Cretaceous avialan bird, *Shenzhouraptor sinensis* from Western Liaoning, China. *Acta Geologica Sinica* **77:** 21–27.

Ji Q, Ji S, Zhang H, You H, Zhang J, Wang L, Yuan C, Ji X. 2002b. A new Avialan bird – *Jixiangornis orientalis* gen. et sp. nov. – from the Lower Cretaceous of Western Liaoning, NE China. *Journal of Nanjing University* **38:** 723–736.

Jiang B, Fürisch FT, Sha J, Wang B, Niu Y. 2011. Early Cretaceous volcanism and its impact on fossil preservation in western Liaoning, NE China. *Palaeogeography, Palaeoclimatalogy, Palaeoecology* **302:** 255–269.

Leduc T. 2012. Les iguanodons de Bernissart : leur évolution diagénétique et les processus de dégradation. DPhil Thesis, University of Liège (Belgium).

Lee M, Worthy T. 2012. Likelihood re-instates *Archaeopteryx* as a primitive bird. *Biology Letters* **8:** 299–303.

Li D, Sullivan C, Zhou Z, Zhang F. 2010. Basal birds from China: a brief review. *Chinese Birds* **1:** 83–96.

Lu J, Xu L, Jiang X, Kia S, Li M, Yuan C, Zhang X, Ji Q. 2009. A preliminary report on the new dinosaurian fauna from the Cretaceous of the Ruyang Basin, Henan province of central China. *Journal of the Paleontological Society of Korea* **25:** 43–56.

Makovicky PJ, Apesteguía S, Agnolín FL. 2005. The earliest dromaeosaurid theropod from South America. *Nature* **437:** 1007–1011.

Marsh OC. 1881. Principal characters of American Jurassic dinosaurs – part V. *American Journal of Science and Arts* **3:** 417–423.

Mayr G, Pohl B, Hartman S, Peters DS. 2007. The tenth skeletal specimen of *Archaeopteryx*. *Zoological Journal of the Linnean Society* **149:** 97–116.

Newesely H. 1989. Fossil bone apatite. *Applied Geochemistry* **4:** 233–245.

Nixon KC. 2002. *Winclada*, Version 1.00.08. Available at: http://www.cladistics.com/

Norell MA, Clarke JA. 2001. Fossil that fills a critical gap in avian evolution. *Nature* **409:** 181–184.

O'Connor J, Chiappe LM, Bell A. 2011. Pre-modern birds: avian divergences in the Mesozoic. In: Dyke G, Kaiser G, eds. *Living dinosaurs: the evolutionary history of modern birds*. Oxford: Wiley-Blackwell, 39–114.

O'Connor J, Sun C, Xu X, Wang X, Zhou Z. 2012. A new species of *Jeholornis* with complete caudal integument. *Histological Biology* **24:** 29–41.

O'Connor J, Wang X, Sullivan C, Zheng X, Tubaro P, Zhang X, Zhou Z. 2013. Unique caudal plumage of *Jeholornis* and complex tail evolution in early birds. *Proceedings of the National Academy of Sciences of the United States of America* October 7, 2013, doi: 10.1073/pnas.1316979110.

Owen R. 1842. Report on British fossil reptiles. *Report of the British Association for the Advancement of Sciences* **9:** 60–204.

Pu H, Chang H, Lü J, Wu Y, Xu L, Zhang J, Jia S. 2013. A new juvenile specimen of *Sapeornis* (Pygostylia: Aves) from the Lower Cretaceous of Northeast China and allometric scaling of this basal bird. *Paleontological Research* **17:** 27–38.

Seebacher F. 2001. A new method to calculate allometric length-mass relationships of dinosaurs. *Journal of Vertebrate Paleontology* **21:** 51–60.

Sereno PC, Rao C. 1992. Early evolution of avian flight and perching: new evidence from the Lower Cretaceous of China. *Science* **55:** 845–848.

Swisher CC, Wang YQ, Wang XL, Xu L, Wang Y. 1999. Cretaceous age for the feathered dinosaurs of Liaoning China. *Nature* **400:** 58–61.

Turner AH, Pol D, Clarke JA, Erickson GM, Norell MA. 2007. A basal dromaeosaurid and size evolution preceding avian flight. *Science* **317:** 1378–1381.

Turner AH, Makovicky PJ, Norell MA. 2012. A review of dromaeosaurid systematics and paravian phylogeny. *Bulletin of the American Museum of Natural History* **371:** 1–206.

Webster D, Goff G. 1977. Variation in the vertebral column and ribs of songbirds. *Proceedings of the Indiana Academy of Science* **87:** 450–459.

Weishampel DB, Dodson P, Osmólska H. 2007. *The Dinosauria*, 2nd edn. Berkeley, CA: University of California Press.

Wellnhofer P. 2009. Archaeopteryx lithographica*: the icon of evolution*. München: Verlag Dr. Friedrich Pfeil.

Xu X, Norell MA. 2004. A new troodontid dinosaur from China with avian-like sleeping posture. *Nature* **475:** 465–470.

Xu X, You H, Du K, Han F. 2011. An *Archaeopteryx*-like theropod from China and the origin of Avialae. *Nature* **475:** 465–470.

Xu X, Zhang F. 2005. A new maniraptoran dinosaur from China with long feathers on the metatarsus. *Naturwissenschafter* **92:** 173–177.

Xu X, Zhao Q, Norell M, Sullivan C, Hone D, Erickson G, Wang X, Han F, Guo Y. 2009. A new feathered maniraptoran dinosaur fossil that fills a morphological gap in avian origins. *Chinese Science Bulletin* **54:** 430–435.

Yang W, Li S, Jiang B. 2007. New evidence for Cretaceous age of the feathered dinosaurs of Liaoning: zircon U-Pb SHRIMP dating of the Yixian Formation in Shietun, northeast China. *Cretaceous Research* **23:** 297–305.

Zhang F, Zhou Z, Xu X, Wang X. 2002. A juvenile coelurosaurian theropod from China indicates arboreal habits. *Die Naturwissenschaften* **89:** 394–398.

Zhang F, Zhou Z, Xu X, Wang X, Sullivan C. 2008. A bizarre Jurassic maniraptoran from China with elongate ribbon-like feathers. *Nature* **455:** 1105–1108.

Zhou Z, Li FZZ. 2010. A new Lower Cretaceous bird from China and tooth reduction in early avian evolution. *Proceedings of the Royal Society of London Series B, Biological Sciences* **277:** 219–227.

Zhou Z, Wang Y. 2010. Vertebrate diversity of the Jehol biota as compared with other lagerstätten. *Science China Earth Sciences* **53:** 1894–1907.

Zhou Z, Zhang F. 2002. A long-tailed, seed-eating bird from the Early Cretaceous of China. *Nature* **418:** 1754–1756.

Zhou Z, Zhang F. 2003a. *Jeholornis* compared to

Archaeopteryx with a new understanding of the earliest avian evolution. *Die Naturwissenschaften* **90:** 220–225.

Zhou Z, Zhang F. 2003b. Anatomy of the primitive bird *Sapeornis chaoyangensis* from the Early Cretaceous of Liaoning, China. *Canadian Journal of Earth Sciences* **40:** 731–747.

Zhou Z, Zhang F. 2006. Mesozoic birds of China – a synoptic review. *Vertebrata Palasiatica* **44:** 74–98.

SUPPORTING INFORMATION

Additional Supporting Information may be found in the online version of this article at the publisher's web-site:

Figure S1. Selected measurements of YFGP-yb2.
Figure S2. Three-dimensional reconstruction of the pelvic region from computed tomography scans.
Figure S3. Energy dispersive spectrometry analysis.
Figure S4. Slices and three-dimensional reconstruction of the ilium in *Jeholornis curvipes.*
Figure S5. Body mass estimation.
Figure S6. Operational taxonomic units added.
Figure S7. Phylogeny.